Polymer 50 (2009) 5708–5712

Contents lists available at ScienceDirect

Polymer

journal homepage: www.elsevier.com/locate/polymer

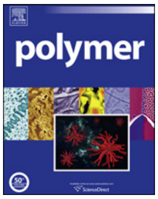

Termination kinetics of free-radical polymerization in ionic liquids

Johannes Barth [a], Michael Buback [a,*], Gudrun Schmidt-Naake [b], Inga Woecht [b]

[a] Institute for Physical Chemistry, University of Göttingen, Tammannstraße 6, D-37077 Göttingen, Germany
[b] Institute of Technical Chemistry, Clausthal University of Technology, Erzstraße 18, D-38678 Clausthal-Zellerfeld, Germany

ARTICLE INFO

Article history:
Received 18 August 2009
Received in revised form
23 September 2009
Accepted 24 September 2009
Available online 2 October 2009

Keywords:
Free-radical polymerization kinetics
Ionic liquids
Electron paramagnetic resonance

ABSTRACT

Termination rate coefficients, k_t, for free-radical polymerization of 15 vol.-% methyl methacrylate (MMA) dissolved in 1-ethyl-3-methylimidazolium bis(trifluoromethylsulfonyl)-imide and in 1-butyl-3-methylimidazolium tetrafluoroborate were measured at 10 °C via the single pulse – pulsed laser polymerization – electron paramagnetic resonance (SP–PLP–EPR) technique. Whereas absolute k_t in ionic liquid solution is by about one order of magnitude below the associated bulk MMA value, the chain-length dependence of k_t is very similar in both liquid environments.

1. Introduction

Ionic liquids (ILs) have found enormous interest during the last decade. ILs consist of a bulky cation and a complex anion and exhibit interesting physical properties such as high thermal and chemical stability as well as negligible vapor pressure which makes them attractive as solvents for environmentally friendly processes. An excellent overview on syntheses and characteristic properties of ILs as well as on their application in transition metal catalysis has been given by Wasserscheid and Keim [1]. Whereas ILs are frequently used as solvents in organic syntheses, applications in free-radical polymerization are scarce. It is however known that polymerization rate and polymer molecular weight in IL solution are enhanced as compared to polymerization in conventional organic solvents or in bulk [2–6], The solvent power of ILs indicates further advantages for copolymerization of monomers which largely differ in polarity [7–9].

PLP-SEC studies into free-radical polymerization of methyl methacrylate (MMA) and glycidyl methacrylate (GMA) showed that the propagation rate coefficient, k_p, is increased for polymerization in IL solution as compared to bulk or solution polymerization in conventional organic solvents [10–12], The increase in k_p is essentially due to polar interactions which lower the activation energy, $E_A(k_p)$, upon replacing the molecular environment of the transition state structure from bulk methacrylate to a surrounding which primarily consists of IL species.[9,12,13].

In addition to an increase in k_p, Haddleton et al. reported a decrease of termination rate coefficient, k_t, by up to one order of magnitude, in passing from bulk polymerization to reaction in highly viscous solution containing 60 vol.-% 1-butyl-3-methylimidazolium hexafluorophosphate ([bmim] PF_6) [11]. Both rate coefficients, k_p and k_t, thus contribute to an enhancement of polymerization rates in the presence of ILs. To investigate the effect of ILs on k_t in more detail, we decided to study MMA polymerizations in the two ILs: 1-butyl-3-methylimidazolium tetrafluoroborate ([bmim] BF_4) and 1-ethyl-3-methylimidazolium bis(trifluoromethylsulfonyl)imide ([emim] NTf_2). These ILs differ in viscosity, as is indicated by the values extrapolated from ref. [30] for 10 °C: 55.9 cP for [emim] NTf_2 and 171 cP for [bmim] BF_4.

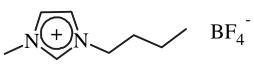

[bmim] BF_4

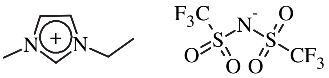

[emim] NTf_2

EPR spectroscopy is perfectly suited for k_t analysis, as the concentration of radicals may be directly and quantitatively measured. The termination rate law (Equation (1)) reads:

$$\frac{dc_R}{dt} = -2\cdot k_t \cdot c_R^2 \tag{1}$$

The SP–PLP–EPR (single pulse–pulsed laser polymerization–electron paramagnetic resonance) method offers particular advantages for k_t determination: The decay of the intense radical concentration produced by a laser single pulse is monitored [14]. As

---

[*] Corresponding author. Fax: +49 551 39 3144.
E-mail address: mbuback@gwdg.de (M. Buback).

0032-3861/$ – see front matter © 2009 Elsevier Ltd. All rights reserved.
doi:10.1016/j.polymer.2009.09.065

radical chain length scales with time t after firing the laser pulse, time-resolved measurement of radical concentration, c_R, provides direct access to chain-length dependent termination rate coefficients, $k_t^{i,i}$, which refer to termination of two radicals of more or less identical chain-length, i. Progress in experimental techniques and in the understanding of chain-length dependent termination kinetics has recently been reviewed by Barner-Kowollik and Russell [15]. General agreement has emerged that $k_t^{i,i}$ as a function of chain-length i is best described by the so-called composite model (Equation (2)) [16].

$$\begin{aligned} k_t^{i,i} &= k_t^{1,1} \cdot i^{-\alpha_s} \quad i \le i_c \\ &= k_t^{1,1} \cdot i_c^{-\alpha_s+\alpha_l} \cdot i^{-\alpha_l} = k_t^0 \cdot i^{-\alpha_l} \quad i > i_c \end{aligned} \tag{2}$$

The model accounts for the pronounced chain-length dependence of k_t at smaller radical size and for the weaker chain-length dependence of radicals with chain length above a crossover value, i_c. The exponent α_s for the short-chain regime is between 0.50 and 1.0 depending on the type of monomer. Crossover chain lengths have been reported to be between 20 and 30 for acrylate monomers [17,18] and up to about 100 for methacrylates [19,20,27] The power-law exponent for long-chain radicals, α_l, has mostly been found to be close to the theoretically predicted value of $\alpha_l = 0.16$ [21–23] or slightly higher. The fourth parameter accessible from SP–PLP–EPR is $k_t^{1,1}$, the rate coefficient for termination of two radicals of chain length unity. To correlate radical chain-lengths with time t after laser pulsing, the propagation rate coefficient, k_p, under the conditions of the SP–PLP–EPR experiment needs to be known. These k_p values are available from the IUPAC-recommended PLP-SEC technique [24].

An intrinsic experimental problem with EPR spectroscopic investigations of highly polar materials is dielectric loss, which may be partially overcome by using small sample sizes. The polarity of ILs is associated with a higher viscosity than the one of typical monomers, which results in a lower k_t and in a higher stationary radical concentration and thus better signal-to-noise quality of the EPR spectrum measured in IL solution.

As has recently been shown, EPR signal quality may be further enhanced by studying MMA-d_8 rather than MMA polymerization [25]. Deuterium exhibits a much weaker coupling to the unpaired electron than protons which results in a decrease of EPR-line splitting by $a_D/a_H \sim 1/6.5$ [26]. At the EPR instrumental settings of our SP–PLP–EPR studies, e.g., at short sweep times, the EPR spectrum consists of one single broad line for radicals occurring in the polymerization of MMA-d_8.

2. Experimental

2.1. Chemicals

MMA-d_8 (99%, stabilized with hydroquinone, Deutero) was purified by passing through a column filled with inhibitor remover (Aldrich). The ILs [bmim] BF_4 (purum ≥ 98%, Lot-No.: 99/602, 402 ppm Cl^-; 622 ppm H_2O, Solvent Innovation GmbH) and [emim] NTf_2 (99%, Lot-No.: F00610.1, <100 ppm halides, <100 ppm H_2O, Iolitec) were used as received. Dissolved oxygen was removed by several freeze-pump-thaw cycles. Also the photoinitiator, α-methyl-4(methylmercapto)-α-morpholino propiophenone (MMMP, 98%, Aldrich), was used as received.

2.2. PLP-SEC experiments

Laser pulsing was carried out with an excimer laser (LPX 210i, Lambda Physik) operated on the 351 nm (XeF) line. A pulse repetition rate of 10 Hz was selected. Polymerizations were carried out in a 65Q cell (Starna, with a jacket for temperature control) with 10 mm path length. MMMP was used at initial concentrations of $6.3 \cdot 10^{-3}$ mol L^{-1}. The monomer solution was purged with nitrogen for about 3 min and sealed with a PTFE cap. Prior to pulsing at 40 °C, the polymerization cell was thermostated for about 15 min. Between 700 and 1000 pulses were applied to reach a monomer conversion of about 5%. After pulsing, the reaction solution was poured into a solution of hydroquinone in methanol for polymer precipitation. Methanol was separated by filtration. The polymer sample was washed with water to remove residual ionic liquid and then dried under vacuum.

2.3. Size-exclusion chromatography

MWDs were determined by means of size-exclusion chromatography using a Waters 515 HPLC pump, Waters 2410 refractive index detector, PSS-SDV columns with nominal pore sizes of 10^5, 10^3, 10^2 Å and THF at 35 °C as the eluent. The SEC setup was calibrated with low dispersity poly(methyl methacrylate) (PMMA) standards for the molecular weight range 410 to 2,000,000 g mol^{-1} (PSS).

2.4. EPR monitoring

The EPR spectra were recorded on a Bruker Elexsys E 500 series cw-EPR spectrometer for sample volumes of 0.05 mL contained in quartz tubes of 3 mm outer and 2 mm inner diameter. The tubes were fitted into the resonator cavity equipped with a grid through which the sample was irradiated with a COMPex 102 excimer laser (Lambda Physik) at an energy of about 70 mJ per pulse. The EPR spectrometer and the laser source were synchronized by a pulse generator (Scientific Instruments 9314). Temperature control was achieved via an ER 4131VT unit (Bruker) by purging the sample cavity with nitrogen. MMMP was added to the degassed monomer in a glove box under an argon atmosphere at initial concentrations of about $3 \cdot 10^{-2}$ mol L^{-1}. The EPR tube was sealed with a plastic cap and with Parafilm and was protected from light prior to PLP.

An EPR spectrum was taken under pseudo-stationary PLP initiation conditions. This spectrum serves for identification of the peak maximum position for subsequent time-resolved measurement. A short sweep time of 10.5 s was selected to avoid significant monomer-to-polymer conversion prior to the SP experiment. In case of polymerization in [bmim] BF_4, no such initial spectrum was recorded, as a faster reaction occurs with this IL which may lead to earlier inhomogeneity because of polymer content. Via the cw-EPR spectra, the modulation amplitude and the microwave energy (to avoid saturation) were optimized to 5 G and 6 mW, respectively. Time-resolved EPR intensity after SP application was measured at the field position of maximum intensity. Absolute radical concentration is obtained via the calibration procedure described elsewhere [27].

2.5. Data fitting

Chain-length averaged termination rate coefficients were obtained from fitting measured $c_R^0/c_R(t)$ vs. t data to Eq. (3), which results from integration of Eq. (1) by assuming chain-length independent k_t. The EPR data refer to chain-length region $i = 1$ to $i_{max} = k_p \cdot t_{max} \cdot c_M + 1$, with t_{max} being the maximum time t, after firing the laser single pulse at $t = 0$, where c_R may be determined with reasonable accuracy. The chain-length regime underlying a particular mean value of the termination rate coefficient, $\langle k_t \rangle$, is indicated by subscript numbers for i and i_{max}.

$$\frac{c_R^0}{c_R(t)} = 1 + 2\langle k_t \rangle_{1,i_{max}} \cdot c_R^0 \cdot t \tag{3}$$

The composite model parameters, $k_t^{1,1}$ and α_s, have been obtained by fitting the EPR data to Eq. (4), which has been derived by Smith and Russell [28] from Eq. (1) assuming power-law behavior for $k_t^{i,i}$:

$$\frac{c_R^0}{c_R(t)} - 1 = \frac{2\cdot k_t^{1,1}\cdot c_R^0\cdot\left[\left(k_p\cdot c_M\cdot t+1\right)^{1-\alpha_s}-1\right]}{k_p\cdot c_M\cdot(1-\alpha_s)} \qquad (4)$$

The fitting to Eq. (4) within the time interval associated with the chain-length range $1 < i < 100$ has been performed in two ways: (a) each data set consisting of several hundred co-added $c_R^0/c_R(t)$ vs. t traces was fitted to yield the parameters $k_t^{1,1}$ and α_s; (b) the arithmetic mean value of the so-obtained α_s (for a given IL) was used for a second fitting of the set of individual $c_R^0/c_R(t)$ vs. t traces. The purpose of this procedure was to deduce $k_t^{1,1}$ values which are less affected by the scatter of α_s.

3. Results and discussion

Shown in Fig. 1 are EPR spectra recorded under excimer laser pulsing, with a pulse repetition rate of 20 Hz, during an MMA-d_8 bulk polymerization at 6 °C and during a solution polymerization with 15 vol.-% MMA-d_8 in [emim] NTf$_2$ at 10 °C.

The higher EPR intensity for polymerization in IL solution reflects the pseudo-stationary radical concentration being higher than in bulk polymerization. Calibration of the spectra in Fig. 1 yields the pseudo-stationary radical concentrations $4.5\cdot10^{-6}$ mol L^{-1} and $6\cdot10^{-7}$ mol L^{-1} during MMA-d_8 polymerizations in IL solution and in bulk, respectively. Under stationary-state conditions and identical initiation rate, this approximately 8-fold enhancement of radical concentration would correspond to a 60-fold lower termination rate coefficient for solution polymerization of 15 vol.-% MMA in [emim] NTf$_2$ as compared to bulk MMA polymerization. As the viscosity of pure MMA is by about a factor of 80 below the one of pure [emim] NTf$_2$ under otherwise identical conditions [29,30], this reduction in termination rate coefficient is close to the expected value, if one assumes k_t to scale with the inverse of viscosity.

Before presenting the SP–PLP–EPR data, propagation rate coefficients, k_p, will be reported for the conditions under which time-resolved EPR experiments have been carried out. The k_p values are required for correlation of radical chain length i with time t after firing the laser pulse. The PLP-SEC experiments have been carried out at 40 °C, as no PLP-structured MWDs could be obtained for 10 °C, where the SP–PLP–EPR experiments have been performed. The rate coefficient measured in [emim] NTf$_2$, $k_p(40\ °C) \approx 1419$ L mol^{-1} s^{-1}, is by about a factor 3 above the associated MMA bulk value [24]. An even larger value, $k_p \approx 1843$ L mol^{-1} s^{-1}, was determined for the solution polymerization of 20 vol.-% MMA in [bmim] BF$_4$. The enhanced k_p is most likely due to intermolecular interactions between MMA and [bmim] BF$_4$. Strehmel et al. observed a clear EPR-line broadening and increased coupling constants for radicals in ionic liquids and assigned this effect to polar radical–solvent interactions [31]. The EPR spectrum of MMA in [emim] NTf$_2$ exhibits some line broadening (Fig. 1) which may be due to hydrogen bonds between the aromatic protons of the imidazolium cation and the oxygen atom of the MMA carbonyl group. The k_p value for MMA-d_8 in [emim] NTf$_2$ at 10 °C has been estimated from the 40 °C value by adopting $E_A(k_p)$ of MMA bulk polymerization. The corresponding estimate of k_p at 10 °C for MMA-d_8 in [bmim] BF$_4$ was performed via the known activation energy for MMA in [bmim] BF$_4$ [12]. The resulting propagation rate coefficients in IL solution at 10 °C are: $k_p/(\mathrm{L\,mol^{-1}\,s^{-1}}) = 870$ and 571 for 15 vol.-% MMA in [bmim] BF$_4$ and in [emim] NTf$_2$, respectively.

Shown in Fig. 2 is the decay of radical concentration, relative to the maximum value of pulsed laser induced radical concentration at $t = 0$, measured by EPR during polymerization of 15 vol.-% MMA-d_8 in both [bmim] BF$_4$ and [emim] NTf$_2$ solution. The SP–PLP–EPR experiment is carried out at the magnetic field associated with maximum EPR intensity, see Fig. 1.

Fitting the SP–PLP–EPR traces to Equation (3) affords for no adequate representation of the experimental data, which supports previous findings of k_t being strongly chain-length dependent at small values of i. The parameter obtained from fitting the decay in radical concentration to Equation (3) is chain-length averaged $<k_t>_{1;100}$ with the subscripts indicating the underlying chain-length region $1 \le i \le 100$ (Table 1).

The rate coefficients $<k_t>_{1;100}$ for MMA-d_8 in both ILs are well below the associated $<k_t>$ value measured for MMA bulk polymerization via the SP–PLP–NIR technique [32]. The direction of change with $<k_t>_{1;100}$ agrees with the one of the inverse of the bulk viscosities at 10 °C: 0.67 cP for MMA, [29] 55.9 cP for dry [emim]

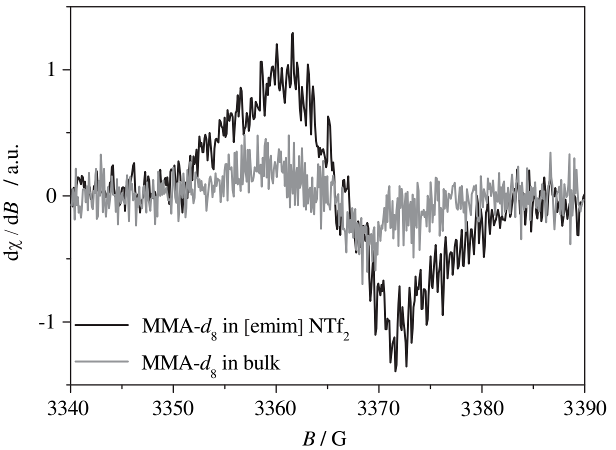

Fig. 1. EPR spectra recorded at a laser pulse repetition rate of 20 Hz during polymerization of MMA-d_8 in bulk at 5 °C (grey line) and in [emim] NTf$_2$ solution (15 vol.-% MMA-d_8) at 10 °C (black line). The spectra were obtained by field sweeps of 10.5 s, a modulation amplitude of 5 G, a time constant of 0.01 ms, and a microwave power of 6 mW.

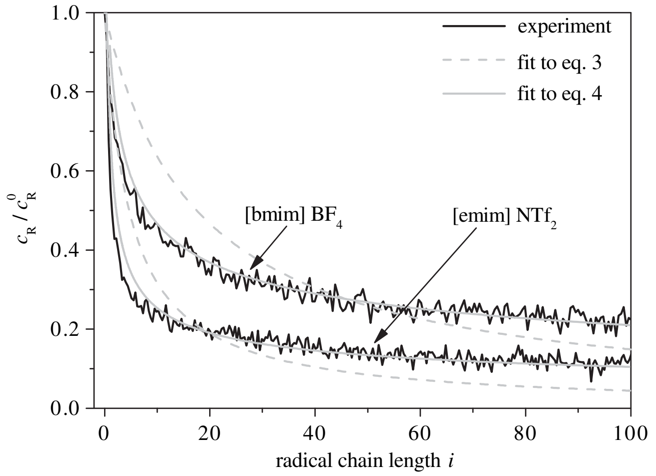

Fig. 2. Decay of relative radical concentration after applying a laser single pulse to MMA-d_8 solutions in [bmim] BF$_4$ and [emim] NTf$_2$. Plotted on the abscissa is chain length i, which scales with time t after firing the SP according to: $i = k_p\cdot c_M\cdot t + 1$. The measured time-resolved EPR traces are represented by the black lines. Fits to Equation (3), that is assuming chain-length independent k_t, are indicated by the dashed grey lines. The Predici-assisted simulation of radical concentration vs. chain length on the basis of chain-length dependent k_t (Equation (4)) is given by the full grey lines.

Table 1
Chain-length averaged termination rate coefficients, $<k_t>_{1;100}$, for MMA solution polymerization (15 vol.-% MMA-d_8) at 10 °C in the two ILs. The data for MMA bulk polymerization are from SP–PLP–NIR studies [32].

Solvent	$<k_t>_{1;100}$/L mol^{-1} s^{-1} for ILs $<k_t>_{1;1000}$/L mol^{-1} s^{-1} for bulk	Reference
[bmim] BF$_4$	$(2.4 \pm 0.1) \times 10^6$	This work
[emim] NTf$_2$	$(7.2 \pm 0.3) \times 10^6$	This work
MMA	2×10^7	[33]

NTf$_2$ and 171 cP for dry [bmim] BF$_4$ (with the numbers for the two ILs extrapolated from ref. [30]). As the viscosity of MMA–IL solutions is strongly affected by moisture [30] and by adding small amounts of organic solvents (here MMA) [33] and as the variation of bulk viscosity with the degree of monomer conversion is not known, no attempt is made to quantitatively correlate $<k_t>_{1;100}$ with inverse bulk viscosity. Another reason for not focusing too much on $<k_t>_{1;100}$ is that this quantity is not well defined and depends on the chain-length range and on the radical concentration profile of the underlying experiment.

A significantly better fit of the experimental SP–PLP–EPR traces is achieved by fitting to Equation (4) (full grey lines in Fig. 2). The resulting composite model parameters, α_s and $k_t^{1,1}$, are plotted vs. final MMA conversion, X, in Fig. 3 and Fig. 4, respectively. The conversion X has been gravimetrically estimated.

Within the limits of experimental uncertainty, the power-law exponent is insensitive toward monomer conversion. It should, however, be noted that X has always been below 20%. The exponent appears to be slightly higher, $\alpha_s = 0.72 \pm 0.05$, for polymerization of 15 vol.-% MMA in [emim] NTf$_2$ than in [bmim] BF$_4$, where $\alpha_s = 0.61 \pm 0.10$ is obtained as the mean value. Averaging the entire set of α_s values measured the two ILs, yields $\alpha_s = 0.66 \pm 0.15$. This number is close to the mean value of $\alpha_s = 0.63 \pm 0.15$ deduced from SP–PLP–EPR studies into MMA-d_8 bulk polymerization at temperatures between 5 and 70 °C [25]. By RAFT-CLD-T experiments, $\alpha_s \approx 0.65$ has been obtained for MMA bulk polymerization at 80 °C [20]. SP–PLP–EPR experiments into the bulk polymerization of other alkyl methacrylates [19,27] resulted in $\alpha_s = 0.65 \pm 0.15$ for n-butyl methacrylate at temperatures between −30 and 60 °C, in $\alpha_s = 0.56 \pm 0.15$ for *tert*-butyl methacrylate at temperatures between −30 and 60 °C, and $\alpha_s = 0.64 \pm 0.07$ for dodecyl methacrylate at temperatures between −20 and 0 °C. A lower value of $\alpha_s = 0.50 \pm 0.07$ has been deduced from SP–PLP–EPR studies into benzyl methacrylate and cyclohexyl methacrylate between −20 and 0 °C.

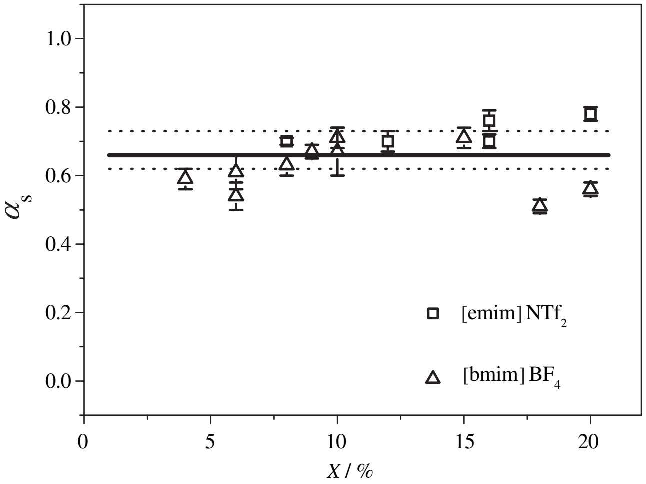

Fig. 3. Power-law exponent α_s for the chain-length region $1 \le i \le 100$ plotted as a function of final monomer conversion for MMA solution polymerizations (15 vol.-% MMA) in [bmim] BF$_4$ (triangles) and [emim] NTf$_2$ (squares). The numbers are deduced from fitting experimental SP–PLP–EPR traces to Equation (4). The dotted lines represent the mean values of α_s for each IL with the higher value referring to [emim] NTf$_2$. A mean value of $\alpha_s = 0.66$ (full line) is obtained by averaging over the entire α_s data set for the two ILs.

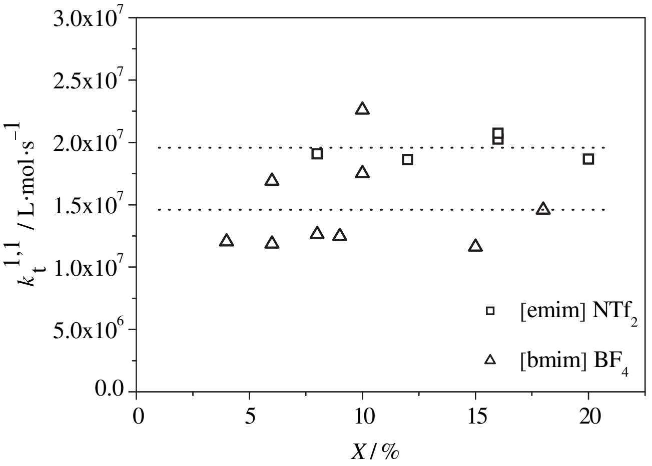

Fig. 4. Termination rate coefficient $k_t^{1,1}$, obtained from fitting the experimental SP–PLP–EPR data to Equation (4). For each IL, the mean value of α_s given in Fig. 4, has been used for fitting $k_t^{1,1}$. The arithmetic mean values of $k_t^{1,1}$ obtained for MMA solution polymerization at 40 °C in [bmim] BF$_4$ (triangles) and [emim] NTf$_2$ (squares) are indicated by dotted lines with the higher value referring to [emim] NTf$_2$.

That more or less the same α_s value applies for MMA bulk polymerization and solution polymerization in ILs, indicates that this power-law exponent is primarily dependent on the type of monomer, but not on molecular environment. This is also suggested by the fact that α_s is insensitive toward polymerization temperature and degree of monomer conversion (and thus polymer content). The family-type behavior of α_s is further supported by the fact that no clear difference is seen between α_s for the smallest (MMA) and largest (dodecyl methacrylate) member of the methacrylate family. In view of this similarity and of the currently available accuracy for α_s determination no justification is seen for arguing about the minor differences between the α_s values for MMA k_t in the two ILs.

For methacrylates with larger alkyl ester side chain, such as butyl or dodecyl methacrylate, in addition to α_s, the power-law exponent α_l, which represents the chain-length dependence of termination rate of radicals with chain lengths $i > i_c$ could be measured via SP–PLP–EPR. Such experiments are difficult to be performed with MMA, where termination is much faster than with butyl and dodecyl methacrylate under otherwise identical conditions. As a consequence, radical concentration decays rapidly after laser pulsing in MMA polymerization, which poses problems toward reliably measuring changes in radical concentration at larger times t after firing the pulse, where the chain length i is large.

The second parameter obtained from fitting the SP–PLP–EPR traces to Equation (4) is $k_t^{1,1}$, the rate coefficient for termination of two MMA radicals both of chain length unity. The entire set of termination rate data has been measured in the initial monomer conversion range where chain-length averaged termination rate coefficients, $<k_t>$, exhibit a plateau-type behavior that suggests k_t to be independent of conversion [32]. It thus appears justified to identify $k_t^{1,1}$ with the arithmetic mean of the $k_t^{1,1}$ values obtained at different (moderate) degrees of monomer conversion for each IL. The fitting has been carried out by adopting the associated power-law exponent, α_s, represented by the corresponding dashed line value in Fig. 3, i.e., $\alpha_s = 0.72$ for MMA polymerization in [emim] NTf$_2$ and $\alpha_s = 0.61$ for MMA polymerization in [bmim] BF$_4$. The so-obtained $k_t^{1,1}$ values for solution polymerization in the two ILs at 10 °C are plotted in Fig. 4. In spite of the scatter of the individual $k_t^{1,1}$, the numbers for [bmim] BF_4 appear to be slightly lower, which is also indicated by the arithmetic mean values of $k_t^{1,1} = (2.0 \pm 0.5) \cdot 10^7\ \mathrm{L\,mol^{-1}\,s^{-1}}$ and $k_t^{1,1} = (1.5 \pm 0.5) \cdot 10^7\ \mathrm{L\,mol^{-1}\,s^{-1}}$ for MMA polymerization in solution of [emim] NTf_2 and [bmim] BF_4, respectively.

The associated MMA-d_8 bulk polymerization value for 10 °C has been determined in a recent SP–PLP–EPR study [25] to be: $k_t^{1,1} \approx 5.1 \cdot 10^8\ \mathrm{L\,mol^{-1}\,s^{-1}}$. The bulk value thus exceeds $k_t^{1,1}$ in [emim] NTf_2 and [bmim] BF_4 solutions (containing 15 vol.-% MMA) by factors of 26 and 34, respectively. Solution viscosity of 15 vol-% MMA in [bmim] BF_4 at 25 °C may be estimated from data reported in Ref. [33] to be 25.8 cP, which is about a factor of 48 above the pure MMA viscosity at the same temperature In view of the fact that the temperature dependence of viscosity is larger for ILs than for MMA [30], that viscosity is difficult to be precisely measured in IL solution even at low degrees of monomer conversion, and that trace amounts of water may affect viscosity, the observed changes in $k_t^{1,1}$ together with the estimated solution viscosities are strongly indicative of the variation in $k_t^{1,1}$ for MMA polymerization in bulk and in solution being mostly determined by the associated change in (inverse) viscosity: $k_t^{1,1}(\text{bulk})/k_t^{1,1}(\text{IL solution}) \approx \eta(\text{IL solution})/\eta(\text{bulk})$ for MMA polymerization at low degrees of monomer conversion and otherwise identical conditions. This finding is in line with the understanding that $k_t^{1,1}$ scales with both the hydrodynamic radius and the inverse of viscosity [27]. As the comparison is made between bulk and solution experiments of the same monomer, the hydrodynamic radius as well as the capture radius should be same and differences in $k_t^{1,1}$ should primarily result from differences in viscosity.

The relevant viscosity for correlation with $k_t^{1,1}$ is the one of the monomer and of the monomer-IL mixture prior to polymerization. The plateau-type behavior in the early period of MMA polymerization, but also of other methacrylates and of styrene, indicates that diffusion controlled termination under such conditions is not affected by the presence of polymer coils. The reason for this insensitivity most likely is that the polymer content is not sufficiently high as to significantly enhance viscosity by coil entanglement. With small radicals, e.g., the ones with chain lengths $i < i_c$, the conversion range where polymer content has only a minor influence on diffusion controlled termination may be even further extended, as these short-chain radicals are not prone to get entangled.

The decay of radical concentration is too fast with MMA as to allow for an accurate SP–PLP–EPR determination of $k_t^{i,i}$ at chain lengths above i_c. To estimate $k_t^{i,i}$ for larger size MMA radicals, the following procedure appears recommendable: $k_t^{i,i}$ is measured for $i < i_c$, e.g., by SP–PLP–EPR, or is estimated from the $k_t^{1,1}$ and α_s parameters for bulk MMA or for any MMA solution polymerization with $k_t^{1,1}$ being adjusted for the particular solvent environment by measuring viscosity. The crossover chain length may be adopted from MMA bulk polymerization, and the subsequent decay of $k_t^{i,i}$ may be estimated via the theoretical value for the chain-length dependence of larger chains, $\alpha_l = 0.16$. It appears to be a matter of priority to check via SP–PLP–EPR experiments for further systems, whether the suggested procedure allows for reasonable estimates of chain-length dependent rate coefficients $k_t^{i,i}$ at low and moderate degrees of monomer conversion.

4. Conclusions

The SP–PLP–EPR technique has been applied toward investigations into the termination rate for free-radical polymerization of MMA dissolved in two ionic liquids. The termination rate in the solvents [emim] NTf_2 and [bmim] BF_4 is considerably slower than in bulk MMA polymerization. As compared to bulk polymerization, the chain-length averaged termination rate coefficient decreases by factors of 3 and 10 for MMA polymerization in 85 vol.-% [emim] NTf_2 and 85 vol.-% [bmim] BF_4 at 10 °C, respectively. The power-law exponent α_s for the chain-length dependence of short MMA radicals in IL solution is more or less identical to the exponent measured for MMA bulk polymerization, whereas the composite model parameter $k_t^{1,1}$ appears to scale with the inverse of solution viscosity.

Acknowledgements

Financial support by the *Deutsche Forschungsgemeinschaft* within the European Graduate School ‘Microstructural Control in Free-Radical Polymerization’ (GRK 585) and a fellowship from the *Fonds der Chemischen Industrie* (J.B.) are gratefully acknowledged. The authors are grateful to Prof. F. Meyer (Institute for Inorganic Chemistry, University of Göttingen) for providing the opportunity of using the EPR spectrometer in his laboratory.

References

[1] Wasserscheid P, Keim W. Angew Chem Int Ed 2000;39. 3772-89.
[2] Kubisa P. J Polym Sci Polym Chem Ed 2005;43:4675–83. Prog Polym Sci 2004;29:3–12.
[3] Hong K, Zhang H, Mays JW, Visser AE, Brazel CS, Holbrey JD, et al. Chem Commun 2002:1368–9.
[4] Strehmel V, Laschewsky A, Wetzel H, Görnitz E. Macromolecules 2006;39: 923–30.
[5] Zhang H, Hong K, Jablonsky M, Mays JW. Chem Commun 2003:1356–7.
[6] Benton MG, Brazel CS. Polym Int 2004;53:1113–7.
[7] Strehmel V, Laschewsky A, Wetzel H. e-Polymers 2006;011.
[8] Vygodskii YS, Mel'nik OA, Lozinskaya EI, Shaplov AS. Polym Sci B 2005;47:122–6.
[9] Woecht I, Schmidt-Naake G. e-Polymers 2007;100. Macromol Symp 2009; 275–276:219–29.
[10] Harrisson S, Mackenzie SR, Haddleton DM. Chem Commun 2002. 2850-1.
[11] Harrisson S, Mackenzie SR, Haddleton DM. Macromolecules 2003;36:5072–5.
[12] Woecht I, Schmidt-Naake G, Beuermann S, Buback M, García N. J. Polym Sci Part A Polym Chem 2008;46:1460–9.
[13] Schmidt-Naake G, Woecht I, Schmalfuß A, Glück T. Macromol. Symp 2009;275-276:204–18.
[14] Buback M, Egorov M, Junkers T, Panchenko E. Macromol Rapid Commun 2004; 25:1004–9.
[15] Barner-Kowollik C, Russell GT. Prog Polym Sci 2009; doi:10.1016/j.progpolymsci.2009.07.002.
[16] Smith GB, Russell GT, Heuts JPA. Macromol Theory Simul 2003;12:299–314.
[17] Junkers T, Theis A, Buback M, Davis TP, Stenzel MH, Vana P, et al. Macromolecules 2005;38:9497–508.
[18] Buback M, Hesse P, Junkers T, Theis T, Vana P. Aust J Chem 2007;60:779–87.
[19] Buback M, Muller E, Russell GT. J Phys Chem A 2006;110:3222–30.
[20] Johnston-Hall G, Theis A, Monteiro MJ, Davis TP, Stenzel MH, Barner-Kowollik C. Macromol Chem Phys 2005;206:2047–53.
[21] Friedman B, O'Shaughnessy B. Macromolecules 1993;26:5726–39.
[22] Khokhlov AR. Macromol Chem Rapid Commun 1981;2:633–6.
[23] Olaj OF, Zifferer G. Makromolekulare Chemie-Rapid Communications 1982;3: 549–56.
[24] Beuermann S, Buback M, Davis TP, Gilbert RG, Hutchinson RA, Olaj OF, et al. Macromol Chem Phys 1997;198:1545–60.
[25] Barth J, Buback M. Macromol Rapid Commun 2009; doi:10.1002/marc.2009.00.335.
[26] Sullivan PD, Koski WS. J Amer Chem Soc 1962;84:1–4.
[27] Barth J, Buback M, Hesse P, Sergeeva T. Macromolecules 2009;42:481–8.
[28] Smith GB, Russell GT. Z Phys Chem (Munich) 2005;219:295–323.
[29] Stickler M, Panke D, Wunderlich W. Makromol Chem 1987;188:2651–64.
[30] Jacquemin J, Husson P, Padua AAH, Majer V. Green Chem 2006;8:172–80.
[31] Strehmel V, Laschewsky A, Stoesser R, Zehl A, Herrmann WJ. Phys Org Chem 2006;19:318–25.
[32] Buback M, Egorov M, Gilbert RG, Kaminsky V, Olaj OF, Russell GT, et al. Macromol Chem Phys 2002;203:2570–82.
[33] Tian Y, Wang X, Wang J. J Chem Eng Data 2008;53:2056–9.